

REPORT

OPTOELECTRONICS

Double-heterojunction nanorod light-responsive LEDs for display applications

Nuri Oh,^{1*†} Bong Hoon Kim,^{1*} Seong-Yong Cho,^{1*} Sooji Nam,² Steven P. Rogers,¹ Yiran Jiang,¹ Joseph C. Flanagan,¹ You Zhai,¹ Jae-Hwan Kim,¹ Jungyup Lee,³ Yongjoon Yu,³ Youn Kyoung Cho,³ Gyum Hur,³ Jieqian Zhang,⁴ Peter Trefonas,⁴ John A. Rogers,¹ Moonsub Shim^{1†}

Dual-functioning displays, which can simultaneously transmit and receive information and energy through visible light, would enable enhanced user interfaces and device-to-device interactivity. We demonstrate that double heterojunctions designed into colloidal semiconductor nanorods allow both efficient photocurrent generation through a photovoltaic response and electroluminescence within a single device. These dual-functioning, all-solution-processed double-heterojunction nanorod light-responsive light-emitting diodes open feasible routes to a variety of advanced applications, from touchless interactive screens to energy harvesting and scavenging displays and massively parallel display-to-display data communication.

With increasing demands for complex, multifunctional electronics in compact, lightweight format (1, 2), a dual ability to convert electricity into different forms of energy and signals and, conversely, to generate energy and signals from electricity is an attractive feature (3–5). In particular, dual-functioning displays that can simultaneously transmit and receive information through visible light can provide real-time bidirectional communication, allowing unique user and device-to-device interfaces and interactivity. Separate single-function devices (e.g., separate light-emitting diodes (LEDs) with photodetectors) can be integrated into systems that can perform two processes (6), but the design requires twice as many devices and a much more cumbersome fabrication process.

Colloidal quantum dots (QDs) have emerged as an important class of electroluminescent (7–9) and photovoltaic (10–12) materials, and heterostructures of QDs have often enabled these applications. Type I straddling band offset can enhance radiative recombination useful for LEDs, and type II staggered band offset leads to efficient separation of photogenerated carriers. Double-heterojunction nanorods (DHNRs) contain type I heterojunctions between the QD and two sur-

rounding materials, which would have type II band offset by themselves (13, 14). Several advantages of DHNRs as electroluminescent materials have recently been demonstrated, including enhanced light outcoupling due to their anisotropy and independent control over electron and hole-injection processes (15). The latter benefit is especially appealing in that it can also apply to carrier extraction and therefore both charge separation and recombination can be fine-tuned within a single material. Here we show that DHNRs, acting as both charge-separation and recombination centers, can simultaneously enable efficient photocurrent generation and electroluminescence within a single device. With a response time <10 μs, these devices operating under ac bias can detect external light sources while appearing to be continuously emitting bright light. This dual capability can impart multiple, enhanced functionalities in displays.

Figure 1A shows the energy band diagram and outlines the dual functionality of solution-processed DHNR-light-responsive LEDs. Simply changing from forward to reverse bias switches between light-emitting and light-detecting modes. High-resolution aberration-corrected scanning transmission electron microscopy images (Fig. 1, B and C) show structural details of DHNRs identifying CdS, CdSe, and ZnSe down to atomic-column resolution. Electroluminescence characteristics, shown along with solution absorption and photoluminescence (PL) spectra, reveal narrow bandwidth (<30 nm), low turn-on voltage (~1.7 V), and high maximum brightness >80,000 cd/m² (fig. S1). These devices exhibit low bias and high efficiencies at display-relevant brightness (e.g., external quantum efficiency of 8.0% at 1000 cd/m² under 2.5 V bias). As a comparison, a similar wavelength-

emitting QD-LED of the same device structure fabricated under the same conditions exhibits external quantum efficiency of 3.1% at 1000 cd/m² with 3.3 V (fig. S2). Furthermore, a recently demonstrated >30 lumens (lm)/W luminous power efficacy is one of the highest, if not the highest, among all red-emitting organic- and QD-LEDs at the practical luminance of 1000 cd/m² (15).

DHNR-LEDs can also operate as useful photodetectors at zero or under reverse bias. A simple example is demonstrated in which a 10 × 10 pixel array is irradiated by a laser pointer (Figs. 1, D to F). A circuit board is programmed to supply a forward bias to any pixel that detects incident light at zero bias. The signal from the laser pointer is then spatially resolved by the LED array, leading to a “writing” action on the “display.” Movie S1 shows this writing process in real time.

To characterize photodetector capability, especially the contributions of the underlying band offsets, we compared DHNR- and QD-LEDs with the same device structure. Under the same illumination condition, DHNR-LED exhibited more than 20-fold-higher short-circuit current, and the photocurrent-to-dark current ratio of 3 × 10⁴ was an order of magnitude larger (Fig. 2A). The corresponding dark currents are shown in fig. S3. The inset of Fig. 2A shows the incident light power dependence at -2-V bias, demonstrating responsivity of ~22 mA/W for 532-nm irradiation. For a 400-nm excitation, we observed responsivity of ~200 mA/W, a value approaching that of commercial Si photodiodes.

The wavelength dependence of incident-photon-to-current efficiency (fig. S4) follows the absorption spectrum of DHNRs well in the red region near the CdSe band-edge absorption. The faster increase beginning near 450 nm may be arising from the onset of contributions from the hole transport layer with DHNRs facilitating the flow of photogenerated carriers. At shorter wavelengths, we expect absorption in the electron transport layer to contribute, allowing for additional means of improvement through the choice of charge-transport materials. Compared to CdSe-QD photodetectors (i.e., QDs without insulating shell that enhances PL and electroluminescence) (16), DHNR-light-responsive LEDs exhibit a similar and an order-of-magnitude larger response in the red and blue regions, respectively. For the core-shell QD case, the wide-band-gap shell that enhances PL causes a significant barrier for carrier extraction. Removing the shell can enhance photocurrent but drastically degrades electroluminescence. Separate band alignments for electrons and holes designed into DHNRs, on the other hand, facilitate both charge injection and extraction (and block opposite charge carriers), allowing one device to exhibit both efficient light emission and detection.

Further insights on photoresponse can be gained through bias dependence of PL lifetime (fig. S5). As shown in Fig. 2B, QDs exhibit no dependence, whereas DHNRs show increasing PL lifetime with forward bias. It has recently been shown that in QDs with CdS-based shell, PL lifetime can increase with reverse bias because of electron transfer from ZnO/cathode at zero bias

¹Department of Materials Science and Engineering, Beckman Institute for Advanced Science and Technology, Frederick Seitz Materials Research Laboratory, University of Illinois at Urbana-Champaign, Urbana, IL 61801, USA. ²Information Control Device Research Section, Electronics and Telecommunications Research Institute, Daejeon, 305-700, Republic of Korea. ³Department of Chemical and Biomolecular Engineering, University of Illinois at Urbana-Champaign, Urbana, IL 61801, USA. ⁴Dow Electronic Materials, 455 Forest Street, Marlborough, MA 01752, USA. *These authors contributed equally to this work. †Corresponding author. Email: 5nuri.oh@gmail.com (N.O.); mshim@illinois.edu (M.S.)

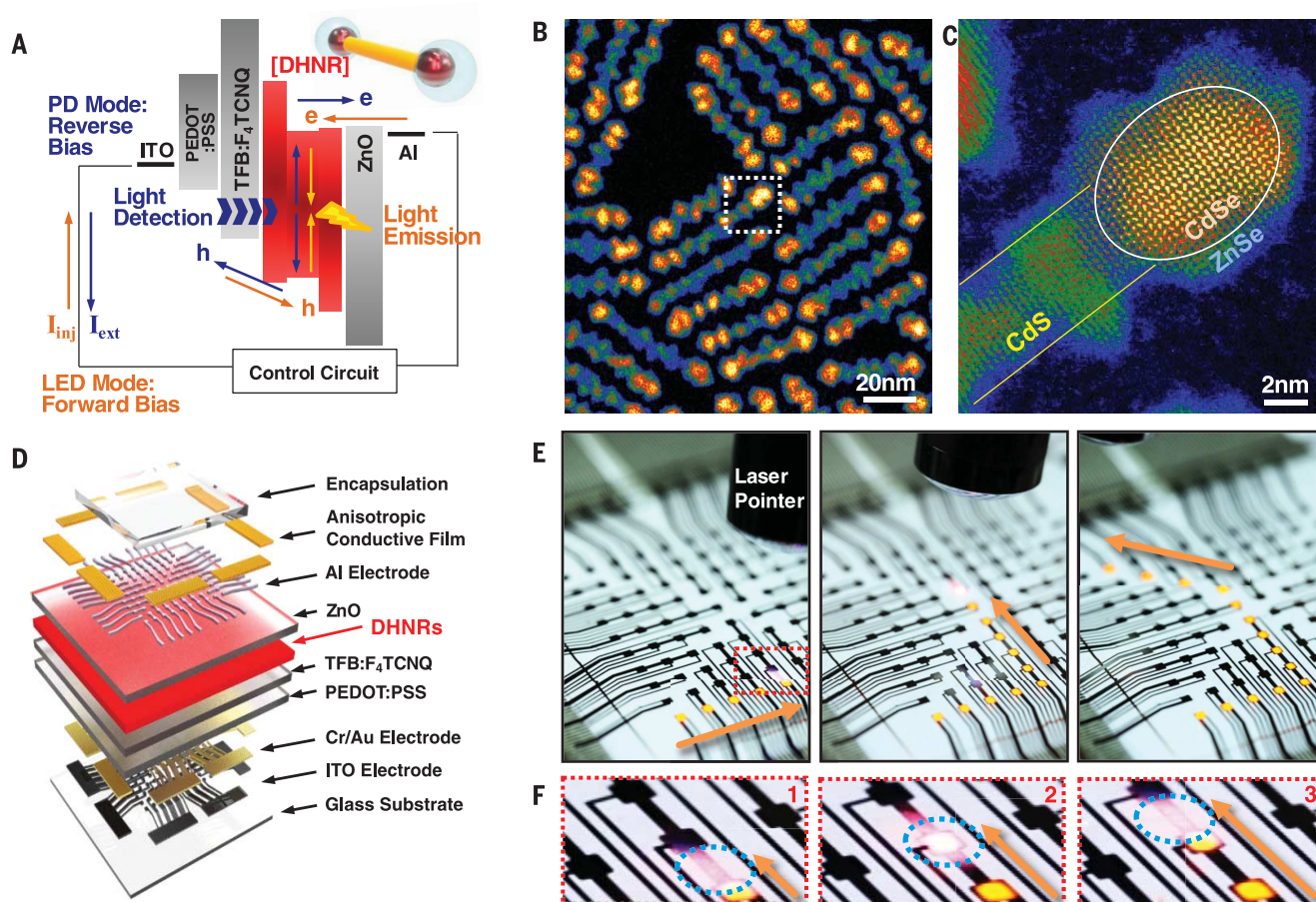


Fig. 1. DHNR–light-responsive LEDs. (A) Energy band diagram of DHNR-LED along with directions of charge flow for light emission (orange arrows) and detection (blue arrows) and a schematic of a DHNR. PD, photodetector; I_{inj} , current injected under LED mode; I_{ext} , current extracted under PD mode; ITO, indium tin oxide; PEDOT:PSS, poly(ethylenedioxythiophene):polystyrene sulfonate; TFB:F₄TCNQ, 2,3,5,6-tetrafluoro-7,7,8,8-tetracyanoquinodimethane-doped poly[(9,9-dioctylfluorenyl-2,7-diyl)-co-(4,4'-(N-(4-sec-butylphenyl)) diphenylamine)]. (B and C) Low- and high-

magnification scanning transmission electron microscopy images of DHNRs, where (C) is a magnified image of the region within the white dotted box in (B). Partial ZnSe growth on the sides helps to enhance PL while maintaining physical access to CdS. (D) Schematic of a 10 × 10 DHNR-LED array. (E) Photographs of a light-responsive LED array with a laser pointer illuminating and turning on pixels along the path outlined by the orange arrows. (F) Magnified images of region enclosed by the red dotted box in (E). Blue dotted circle shows region illuminated by laser pointer.

(17). This charge transfer has been suggested to lead to negative trions upon photoexcitation at zero and small forward bias causing faster PL lifetime, whereas negative bias removes the extra electrons leading to more contribution from neutral exciton recombination and therefore a longer PL lifetime. By using a ZnS-based shell that introduces a barrier for electron transfer, this bias dependence of PL lifetime can be removed (8, 17, 18), and our QDs, which have ZnS shell, show the expected lack of bias dependence. However, DHNRs exhibit completely the opposite behavior of increasing PL lifetime with forward rather than reverse bias. This unexpected dependence is unlikely to be due to DHNRs being positively charged because (i) it is energetically unfavorable based on band alignment and (ii) compared to the “gray” negative trions, positive trions are expected to be dark (19, 20), which would translate to an even lower electroluminescence (opposite to what is experimentally observed). Rather, we believe it is the efficient carrier extraction that leads to this behavior.

This photocurrent contribution is evident when we compare PL lifetime of DHNRs at zero bias and open circuit voltage (V_{oc}) and when the device is electrically floating. At zero bias, we observe PL lifetime of 9 ns. When the device is floating, it doubles to 18 ns (black star in Fig. 2B). This increase is very similar to the case when a forward bias of 1.5 V is applied, which is V_{oc} where the photocurrent goes to zero (Fig. 2A). These results suggest that exciton (and trion, if it existed) recombination time is not altered by the applied potential due to Stark effect. If the bias dependence were to arise from applied field-induced changes to these recombination times, one would expect the PL lifetime when the circuit is opened to be the same as that at zero bias rather than at V_{oc} . When the two electrodes are shorted (for $V < V_{oc}$), photogenerated carriers are extracted and transported away from DHNRs as photocurrent, causing PL lifetime to appear substantially shorter. The application of V_{oc} cancels out the inherent driving force for photocurrent generation, allowing carriers to remain and recombine radi-

tively. When the device is electrically floating, there is also no current flow and, therefore, photo-generated carriers also remain, leading to similar PL lifetime as under V_{oc} . As expected, QDs with ZnS shell, which causes sufficient barriers for charge separation and extraction, do not exhibit such behavior. Hence, it is the double heterojunction designed into DHNRs that simultaneously enhances charge injection and extraction and, therefore, both light emission and detection.

In addition to efficient electroluminescence and photocurrent generation, a fast response is necessary for developing platforms relevant for video displays and practical photodetectors. Transient measurements show that the electroluminescence from a DHNR-LED decays in about 0.8 μ s (Fig. 3A), three orders of magnitude faster than the ~2-ms response of current commercial liquid crystal displays (LCDs). Temporal response in the photodetector mode is also sufficiently fast in the microsecond range. Pulse excitation by a 450 nm commercial LED leads to photocurrent rise and

decay times of ~ 6.5 and ~ 6.6 μs , respectively, at zero bias (Fig. 3B).

By using alternating forward and reverse bias at a submillisecond time scale, fast response times can be exploited to detect signal while appearing to be continuously emitting light to the human eye (movie S2). The photocurrent arising from a green laser (modulated by an optical chopper at 10 Hz) detected under ac operation ($+3/-2$ V with 0.3-ms period) is shown in Fig. 3D. By integrating a simple control circuit, the detected signal can also be translated into a desired response.

For example, brightness can be automatically adjusted in response to external light-intensity change (Fig. 4A and movie S3). The detection and control are at the individual-pixel level that would be especially useful for displays, (e.g., when different parts of the screen are under different lighting conditions). The shadow formed by an approaching finger under room light can also be detected, and the brightness of individual pixels can be adjusted in response (Fig. 4B and movie S4). This sensing ability can enable the design of new touchless user interfaces, as well as direct imaging

with display screens. We note that the long-term stability under this dual-mode ac operation appears promising, with no measurable decrease in brightness and photoresponse over 65 hours of continuous operation at initial luminance of 1067 cd/m^2 and 50% duty cycle (fig. S6). Furthermore, less than 3% change in luminance and 5% in photocurrent were observed upon operation at elevated temperatures up to 60°C.

The dual light-emitting and light-detecting operation with fast response times can also enable direct display-to-display data communication. A proof-of-concept of two identical red-emitting DHNR-LEDs communicating at 10 and 50 kHz is shown in Fig. 4C. At 50 kHz, photocurrent in the receiver does not fully follow the potential applied to the transmitter but is sufficiently saturated and thus can still be read. In this dual mode, a trade-off exists between illumination and communication rate that depends on the duty cycle, but the high brightness of DHNR even at low biases may provide a means of compensating for this trade-off. Although the speeds here are far from established device-to-device communication technologies such as Bluetooth (tens of Mbit/s) and near-field communication (hundreds of kbit/s), this approach has the potential to be made into parallel means of communication using LED arrays that are actual pixels of a display. With recent advances in patterning QDs demonstrating resolution better than 2500 pixels per inch and multi-color pixel arrays on a single substrate with each color having tailored charge transport layers (21, 22), LED displays capable of massively parallel data communication may indeed be feasible. Of course, in order to realize the full potential of massively parallel communication, it would be necessary to maintain an accurate alignment of the corresponding pixels between the displays and to focus the signals in a manner that would reduce dispersion effects to minimize cross-talk.

Finally, photodetection in DHNR-light-responsive LEDs occurs via the photovoltaic effect. Photocurrent generated under air mass (AM) 1.5 illumination (Fig. 4D) leads to power conversion efficiency of 0.2%, which is typical among devices tested, with the highest being 0.3%. Given that there is only about a monolayer of DHNRs and therefore most of the incident photons are not absorbed, there is room for improvement. Furthermore, V_{oc} of 1.49 V is quite high, and, despite the modest efficiency, these light-responsive LEDs are capable of charging a 0.1 F supercapacitor under a halogen microscope illumination lamp (Fig. 4E). The supercapacitor charged by four devices operating in the photovoltaic mode can then be used to power the same devices in the LED mode. That is, displays can be made to harvest or scavenge energy from ambient light sources without the need for integrating separate solar cells.

The dual light-emitting and light-detecting (harvesting) mode of operation with an orders-of-magnitude faster response time than typical display requirements can not only enhance established capabilities but also completely redefine what a display is and how it functions, or, rather, how it can multitask. Displays that can function

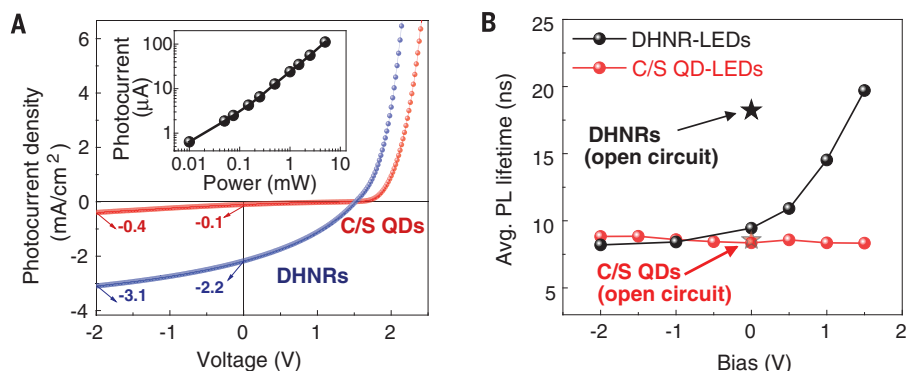


Fig. 2. Photovoltaic characteristics and PL lifetime under bias. (A) Photocurrent under 5-mW, 532-nm excitation for core/shell (C/S) QD- and DHNR-LEDs (red and blue curves, respectively). The inset shows the power dependence for the DHNR-LED. (B) Bias-dependent weighted average PL lifetime of QD- and DHNR-LEDs. Small bias range ensures no contribution from electroluminescence. Open circuits (stars) correspond to measurements when the devices are electrically floating.

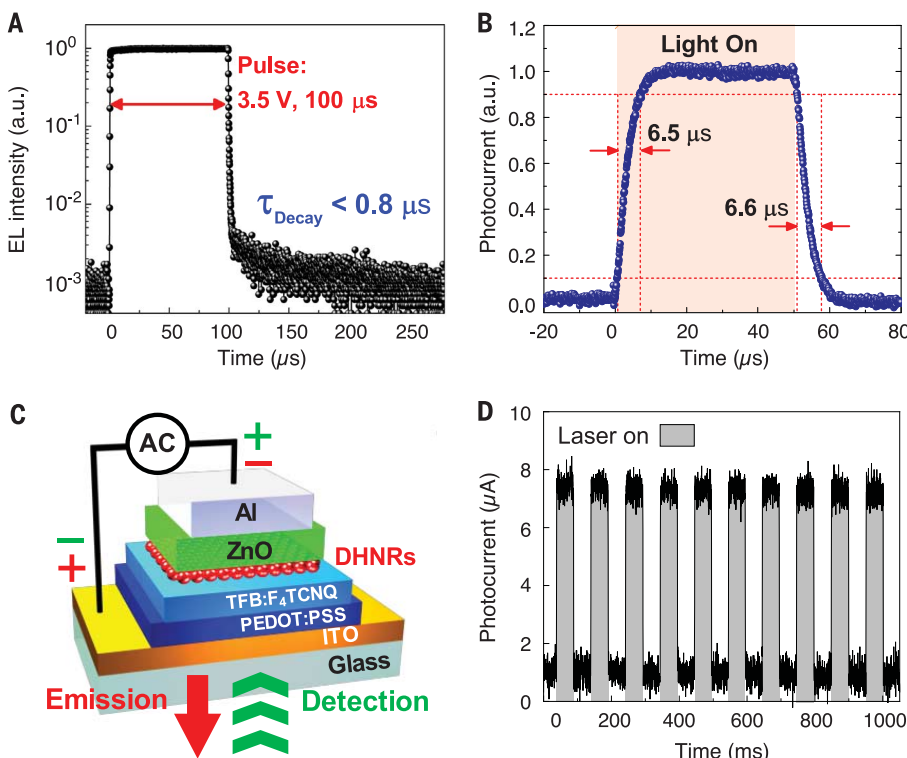


Fig. 3. Temporal response of dual-functioning DHNR-LEDs. (A) Transient electroluminescence (EL) showing decay time (τ_{Decay}); a.u., arbitrary units. (B) Photocurrent in response to illumination by a blue LED source driven by 3 V, 50 μs square-wave voltage pulses. Response time is defined as the time between 10 and 90% of the maximum photocurrent. (C) Schematic of the simultaneous light-emitting and light-detecting operation using ac bias. (D) Photocurrent measured during the dual-mode operation.

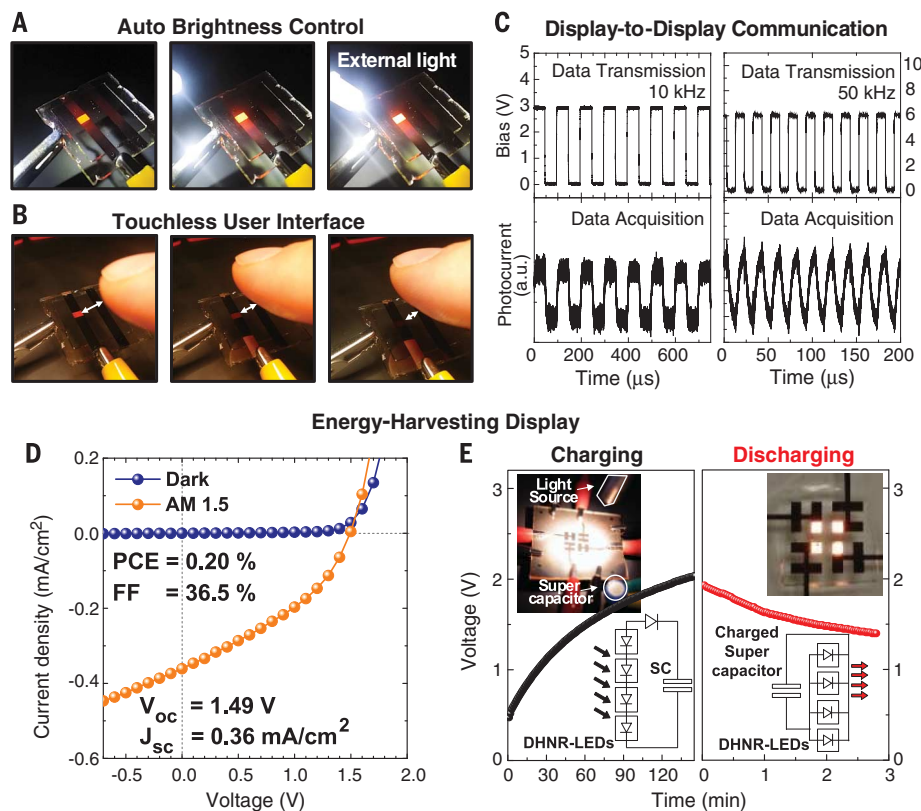


Fig. 4. Proof-of-concept applications of fast light-responsive DHNR-LEDs. (A and B) Automatic brightness control at the single-pixel level in response to an approaching white LED bulb or an approaching finger that blocks ambient light. (C) Demonstration of light-signal generation and detection using two identical DHNR-LEDs; a.u., arbitrary units. (D) Current density versus voltage characteristics of a light-harvesting DHNR-LED under dark and AM 1.5 (100 mW/cm²) conditions. PCE, power conversion efficiency; FF, fill factor; J_{sc} , short-circuit current density. (E) Time-dependent voltage curves of a supercapacitor (SC) being charged by and powering four DHNR-LEDs. Insets show the corresponding circuit diagram and photograph of the LEDs.

as a light-activated electronic whiteboard or a light stylus-responsive tablet would enable new modes of communication, drawing, and artistic creativity. Touchless user interfaces could provide new forms of multifinger or gestural interactivity. In addition to these exciting capabilities, automatic brightness control at the individual pixel level, imaging, massively parallel data communi-

cation, and energy harvesting and scavenging are just a few examples that we have demonstrated the feasibility of here. With versatile solution processability and recent advances in patterning multicolor QDs in ultrahigh resolution (21, 22), one can envision such multifunctional displays consisting of a large array of DHNR-light-responsive LEDs.

REFERENCES AND NOTES

- M. Kaltenbrunner *et al.*, *Nature* **499**, 458–463 (2013).
- J. He, R. G. Nuzzo, J. A. Rogers, *Proc. IEEE* **103**, 619–632 (2015).
- F. J. DiSalvo, *Science* **285**, 703–706 (1999).
- P. Dietz, W. Yezazunis, D. Leigh, in *UbiComp 2003: Ubiquitous Computing* (Lecture Notes in Computer Science Series, Springer, Berlin, 2003), vol. 2864, pp. 175–191.
- D. Tsonev *et al.*, *IEEE Photonics Technol. Lett.* **26**, 637–640 (2014).
- U. Vogel, *et al.*, *SID Symp. Dig. Tec.* **46**, 66 (2015).
- X. Dai *et al.*, *Nature* **515**, 96–99 (2014).
- J. Lim *et al.*, *Adv. Mater.* **26**, 8034–8040 (2014).
- Y. Shirasaki, G. J. Supran, M. G. Bawendi, V. Bulović, *Nat. Photonics* **7**, 13–23 (2012).
- C.-H. M. Chuang, P. R. Brown, V. Bulović, M. G. Bawendi, *Nat. Mater.* **13**, 796–801 (2014).
- P. V. Kamat, *J. Phys. Chem. Lett.* **4**, 908–918 (2013).
- G. H. Carey *et al.*, *Chem. Rev.* **115**, 12732–12763 (2015).
- N. Oh *et al.*, *Nat. Commun.* **5**, 3642 (2014).
- N. Oh, M. Shim, *J. Am. Chem. Soc.* **138**, 10444–10451 (2016).
- S. Nam, N. Oh, Y. Zhai, M. Shim, *ACS Nano* **9**, 878–885 (2015).
- D. C. Oertel, M. G. Bawendi, A. C. Arango, V. Bulović, *Appl. Phys. Lett.* **87**, 213505 (2005).
- W. K. Bae *et al.*, *Nat. Commun.* **4**, 2661 (2013).
- Y. Shirasaki, G. J. Supran, W. A. Tisdale, V. Bulović, *Phys. Rev. Lett.* **110**, 217403 (2013).
- Y.-S. Park, W. K. Bae, J. M. Pietryga, V. I. Klimov, *ACS Nano* **8**, 7288–7296 (2014).
- D. E. Gómez, J. van Embden, P. Mulvaney, M. J. Ferré, H. Rubinsztein-Dunlop, *ACS Nano* **3**, 2281–2287 (2009).
- M. K. Choi *et al.*, *Nat. Commun.* **6**, 7149 (2015).
- B. H. Kim *et al.*, *ACS Nano* **10**, 4920–4925 (2016).

ACKNOWLEDGMENTS

We thank H. Oh for helpful discussions on programming software for the control circuitry. This material is based on work supported by the Dow Chemical Company and the NSF (grant no. DMR-1507170). Experiments were carried out, in part, in the Frederick Seitz Materials Research Laboratory Central Facilities, University of Illinois. N.O., S.N., Y.Z., P.T., and M.S. are inventors on patents US 20150243837 A1, US 8937294 B2, and US 9123638 B2, which are held by the University of Illinois and Dow Chemical and cover the synthesis of double-heterojunction nanorods. N.O., B.H.K., S.-Y.C., P.T., J.Z., J.A.R., and M.S. are inventors on patent applications 62/312629, 62/312633, and 62/312641, which were submitted by the University of Illinois and Dow Chemical and cover the dual light-emitting and light-detecting operation of LEDs and their uses.

SUPPLEMENTARY MATERIALS

www.sciencemag.org/content/355/6325/616/suppl/DC1
Materials and Methods
Figs. S1 to S6
Movies S1 to S4

12 October 2016; accepted 12 January 2017
10.1126/science.aal2038



Double-heterojunction nanorod light-responsive LEDs for display applications

Nuri Oh, Bong Hoon Kim, Seong-Yong Cho, Sooji Nam, Steven P. Rogers, Yiran Jiang, Joseph C. Flanagan, You Zhai, Jae-Hwan Kim, Jungyup Lee, Yongjoon Yu, Youn Kyoung Cho, Gyum Hur, Jieqian Zhang, Peter Trefonas, John A. Rogers and Moonsub Shim
(February 9, 2017)
Science **355** (6325), 616-619. [doi: 10.1126/science.aal2038]

Editor's Summary

Multifunctional displays

As we head toward the "Internet of things" in which everything is integrated and connected, we need to develop the multifunctional technology that will make this happen. Oh *et al.* developed a quantum dot-based device that can harvest and generate light and process information. Their design is based on a double-heterojunction nanorod structure that, when appropriately biased, can function as a light-emitting diode or a photodetector. Such a dual-function device should contribute to the development of intelligent displays for networks of autonomous sensors.

Science, this issue p. 616

This copy is for your personal, non-commercial use only.

Article Tools Visit the online version of this article to access the personalization and article tools:
<http://science.sciencemag.org/content/355/6325/616>

Permissions Obtain information about reproducing this article:
<http://www.sciencemag.org/about/permissions.dtl>

Science (print ISSN 0036-8075; online ISSN 1095-9203) is published weekly, except the last week in December, by the American Association for the Advancement of Science, 1200 New York Avenue NW, Washington, DC 20005. Copyright 2016 by the American Association for the Advancement of Science; all rights reserved. The title *Science* is a registered trademark of AAAS.